Jordan Journal of Physics

REVIEW ARTICLE

Reactor Pressure Vessel Steel Degradation Studied by Mössbauer and Positron Annihilation Spectroscopy

Jozef Lipka

Department of Nuclear Physics and Technology, Slovak University of Technology, Ilkovičova 3, 81219 Bratislava, Slovakia. And Slovak Institute of Metrology, Bratislava, Slovakia.

Abstract: The work applies Mössbauer spectroscopy (MS) and positron annihilation spectroscopy (PAS) to evaluate the microstructure parameters of materials. These methods are used for collecting additional characteristics for understanding the degradation processes in reactor pressure vessel steels. Samples from the Russian 15Kh2MFA and Sv10KhMFT steels, commercially used at WWER-440 nuclear reactors, were irradiated near the core at NPP Bohunice (Slovakia) to neutron fluences in the range 7.8×10^{23} m^{-2} to 2.5×10^{24} m^{-2}. Systematic changes in the MS and PAS spectra were observed mainly during the early period of irradiation. These could be due to changes caused by precipitation of elements like Cu, P or Cr, mainly in carbides, on the surface. The MS results confirm that the close environment of Fe atoms in the b.c.c. lattice of RPV steels remains almost stable after initial changes and can be correlated with the ductile-brittle transition temperature curve from mechanical tests. Positron annihilation lifetime measurements using the Pulsed Low Energy Positron System (PLEPS) were applied for investigation of defects of irradiated and thermally treated reactor pressure vessel (RPV) steels. PLEPS results showed that the changes in the microstructure of the RPV-steel properties caused by neutron irradiation and post-irradiation thermal treatment can be detected in the surface as well as the bulk region.

Keywords: Reactor pressure vessel steels; Mössbauer spectroscopy; Positron annihilation; Neutron irradiation, Neutron embrittlement.

PACS: 81.70.-q, 61.80.Hg, 78.70.Bj

1. Introduction

The degree of embrittlement in a reactor pressure vessel (RPV) is a complex function of different parameters such as temperature, neutron fluence, flux and material chemistry, ect. [1-9]. Many results on embrittlement mechanisms have been obtained on a macroscopic scale and with well proven macroscopic techniques. However, prediction and modeling of the property changes would benefit from knowledge of the evolution of the irradiation-produced microstructure. Therefore, for a good microscopic understanding of the damage caused by radiation, microstructural investigation techniques need to be applied. In order to gain better understanding of the microscopic mechanisms of irradiation embrittlement, Mössbauer and positron annihilation spectra have been collected for a number of selected steel samples within a Slovak extended surveillance specimen program. As-received, thermally treated as well as irradiated conditions have been considered.

Many additional test methods, summarised in Ref.[10] have been developed to unravel the complex microscopic

Corresponding Author: J. Lipka. **Email**: jozef.lipka@stuba.sk.

mechanisms responsible for RPV steel embrittlement. According to our experimental possibilities and practical experiences, the Mössbauer spectroscopy (MS) results were compared mostly with positron annihilation spectroscopy (PAS) [11-26] and transmission electron microscopy (TEM) [18, 20, 24, 27, 28].

2. Application of Mössbauer Spectroscopy to RPV-steel Investigation

Mössbauer spectroscopy (MS) is a powerful analytical technique because of its speciality for one atomic species and because of its extremely high sensitivity to changes in the atomic configuration in the near vicinity of the probe isotopes (in this case ^{57}Fe). MS measures hyperfine interactions and these provide valuable and often unique information about the magnetic and electronic state of the iron species, their chemical bonding to co-ordinating ligands, the local crystal symmetry at the iron sites, structural defects, lattice-dynamical properties, elastic stresses, etc. [30, 31]. In general, a Mössbauer spectrum shows different components if the probe atoms are located at lattice positions, which are not chemically equivalent. From the parameters that characterise a particular Mössbauer sub-spectrum it can, for instance, be established whether the corresponding probe atoms reside in sites which are not affected by structural lattice defects, or whether they are located at defect-correlated positions. In this respect, however, it is imperative to combine Mössbauer measurements with other research methods, which preferably are sensitive to the nature of the defect properties. Combining the results of MS and other techniques [32] on the same samples seems to be a promising approach for such study.

Differences between Mössbauer spectra obtained from different Eastern as well as Western types of RPV steels were already discussed in detail [33, 34]. Only few studies, indicating MS to be a potentially interesting tool to investigate the microstructural aspects of irradiation embrittlement of RPV steels, have been performed so far [29, 31, 33, 34]. The results showed that the distribution analysis of the spectra makes it possible to distinguish between the different steel types. Small differences in carbon concentrations between Western base and weld metal are reflected in the small area fraction of the cementite doublet for the weld metal. Differences between Eastern and Western type RPV steels are reflected in the overall shape of the derived H_{hf}-distribution profile. The larger fraction of the 'perturbed' area for the Eastern steel, the differences in H_{hf} and δ values and the absence of a carbide doublet sub-spectrum are all due to the fact that the overall alloy-element concentration (especially for Cr and V) for the Eastern steels is larger than for Western-type steels. This interpretation was supported also by results from transmission electron microscopy and positron-annihilation measurements [24, 27]. Vanadium carbides (V_xC_y) formation was confirmed also using small angle neutron scattering (SANS) [35, 36]. According to latest knowledge, V is known as a predominant element to enhance the tensile properties of material.

3. Application of the PAS Techniques

Since 1985, positron annihilation spectroscopy (PAS) has been repeatedly used in the study of RPV steels [5, 11-26]. The positron lifetime (PL) technique is a well-established method for studying open-volume type atomic defects and defect-impurity interactions in metals and alloys. The lifetime of positrons trapped at radiation-induced vacancies, vacancy-impurity pairs, dislocations, microvoids, etc. is longer than that of free positrons in the perfect region of the same material. As a result of the presence of open-volume defects, the average positron lifetime observed in structural materials is found to increase with radiation damage [15, 19].

According to previous work it seems to be generally accepted that in RPV steels (containing more than 0.1 wt. % of copper), the copper and phosphorus rich precipitates play a dominant role in thermal and radiation embrittlement [2, 4, 37-39]. In case of Russian-type RPV steels, the formation of carbides has been proposed as an additional micro-structural mechanism derived from comprehensive PAS [11] and transmission

electron microscopy (TEM) studies [27, 28]. Therefore, the main purpose of the present investigation was to look for differences between non-irradiated, annealed, irradiated and post-irradiation thermally treated WWER-440 base and weld RPV materials by means of the unique pulsed low energy positron system (PLEPS).

For the interpretation of results from PL measurements, the standard trapping model (STM) can be used [40], if the sample is homogenous. This premise, however, does not hold for RPV-steels completely. In inhomogeneous samples, the diffusion of positrons from the various implantation sites to the trapping centres has also to be considered [41, 42]. However, the mathematical difficulties associated with the corresponding diffusion-trapping model (DTM) [43], have so far prevented exact solutions in all but the simplest cases [44, 45]. Thus it was impossible to analyse quantitatively the very detailed experimental results obtained with the pulsed positron beam. The application of improved DTM combined with the pulsed positron beam technique is described in detail in [46].

For the first time the pulsed low-energy positron system (PLEPS) [47, 48] was used for the investigation of neutron-irradiated RPV-steels. This system enables the study of the microstructural changes in the region from 20 to 550 nm (depth profiling) with small and very thin (< 50 μm) specimens, therefore reducing the disturbing ^{60}Co radiation contribution to the lifetime spectra to a minimum [26]. Such a disturbance is the limiting factor for the investigation of highly irradiated RPV specimens with conventional positron lifetime systems.

Several approaches to tackle the problem of the ^{60}Co prompt-peak interference with the physical part of the positron lifetime spectra have been considered so far [11, 21, 49, 50]. Besides the PLEPS technique, one of the other acceptable solutions seems to be a triple-coincidence method using a ^{22}Na-source [21]. In this case three γ-rays – one with energy of 1274 keV and two with 511 keV – accompany each event of positron annihilation, while only two γ-rays result from the ^{60}Co decay. However, compared to conventional two-detector systems, the requirement of the triple coincidence reduces drastically the rate of accumulation of positron lifetime spectra [19, 21] and in comparison, PLEPS reduces the measuring time by a factor of 500 and enables in addition the estimation of the defect concentration.

The time resolution of PLEPS was about 240 ps FWHM. All lifetime spectra of irradiated RPV specimens contained about $3×10^7$ events at a peak to background ratio in the range between 30:1 and 100:1 [26].

4. Specimens and irradiation conditions

In the Extended Surveillance Specimen Program (ESSP) 24 specimens, designed especially for MS measurement, were selected and measured in the "as received" state, before their placement into the core of the operated nuclear reactor [25, 51]. The ESSP and specimen preparation are presented in detail in part I of this complex paper. For this program and measurement of high-irradiated RPV-specimens the one-dimensional angular correlation positron-annihilation spectrometer was developed at the Department of Nuclear Physics and Technology of Slovak University of Technology in Bratislava [52]. Results from this measurement are reported in detail in [53]. Beside this, the positron annihilation lifetime spectra were measured using a pulsed low energy positron system at the University of Bundeswehr in Munich (Germany). Both techniques were upgraded for measurement of irradiated specimens, where disturbing ^{60}Co contribution was a limiting factor for measurement in the past. The positron annihilation results were reported in preliminary form [26].

Room temperature Mössbauer spectroscopy measurements were carried out in transmission geometry on a standard constant acceleration spectrometer with a ^{57}Co source in Rh matrix [29]. The absorbers consisted of 25-40 μm thick foils. Due to higher neutron embrittlement and ageing sensitivity of WWER 440 (V-230) nuclear reactors, our study has been focused on the Russian 15Kh2MFA steel used in this older WWER-440 reactor type.

Specimens were measured before their placement into the irradiation chambers, near the core of the operated nuclear reactor, and after 1, 2 and 3 years stay there (neutron fluency in the range 7.8×10^{23} m^{-2} up to 2.5×10^{24} m^{-2}). Taking into account the enhancement of the irradiation due to the closer position of the irradiation chambers to the reactor core ("accelerating" factor of about 10 at the most loaded position), the radiation treatment of the specimens after 3 years is equivalent to about 30 years of real RPV-steel (projected lifetime of RPV). The chemical composition and the irradiation conditions of the studied RPV-steel specimens are shown in Table 1 and Table 2.

TABLE 1. The chemical composition of the RPV-steel specimens [14]. The possible nitrogen concentration is not given in the steel certificate. Nevertheless, we assume its presence approximately at the level of carbon.

| | Chemical composition in wt. % | | | | | | | | | | | |
	C	Si	Mn	S	P	Cr	Ni	Mo	V	As	Co	Cu
BM	0.13-0.18	0.17-0.37	0.30-0.60	max. 0.025	max. 0.025	2.50-3.00	max. 0.40	0.60-0.80	0.25-0.35	max. 0.050	max. 0.020	max. 0.150
Unit 3	0.14	0.22	0.49	0,016	0.013	2,81	0.065	0.615	0.335	0,007	0,009	0.072
Unit 4	0.15	0.24	0.41	0.015	0.015	2.86	0.085	0.7	0.322	0.007	0.007	0.075
WM	0.03-0.12	0.20-0.65	0.55-1.30	max. 0.030	max. 0.030	1.10-1.60	-	0.40-0.60	0.15-0.30	max. 0.050	max. 0.025	max. 0.120
Unit 3	0.042	0.64	1.22	0.015	0.013	1.32	-	0.44	0.24	-	0.003	0.10
Unit 4	0.031	0.60	1.13	0.015	0.010	1.31	-	0.52	0.19	-	0.006	0.06

TABLE 2. Description of the specimens irradiated at the 3rd unit of NPP Bohunice (Slovakia) during 1995-1998.

Sample	Material	Time of irradiation (eff. days)	Neutron Fluence ($E_n > 0.5$ MeV) (m^{-2})	Total activity (kBq)	Thickness of sample (μm)
ZMNF	Base metal non-irradiated	0	0	0	60
ZM1Y	Base metal 1 year irradiated	280	7.81E23	62	50
ZM2Y	Base metal 2 year irradiated	578	1.64E24	109	40
ZM3Y	Base metal 3 year irradiated	894	2.54E24	89	30
ZMNA	Sample ZMNF annealed 1 hour in vacuum at 385°C	0	0	0	60
ZKNF	Weld non-irradiated	0	0	0	55
ZK1Y	Weld 1 year irradiated	280	7.81E23	30	45
ZK2Y	Weld 2 years irradiated	578	1.64E24	48	25
ZK3Y	Weld 3 years irradiated	894	2.54E24	110	47
ZKNA	Sample ZKNF annealed 1 hour in vacuum at 385°C	0	0	0	60

The temperature during the irradiation was measured, using melting monitors (special materials with well-defined melting temperature) placed inside special containers, and reached values in the region of 285-298 °C. Neutron monitors measured the level of the neutron fluence.

5. Results

5.1. MS Results

Mössbauer spectra, which correspond to the basic and weld material samples, show typical behaviour of dilute iron alloys and can be described with three [23] or four sextets (this work). The reference MS spectra were compared with the irradiated state of identical specimens. These specimens were placed into operated nuclear reactor in the NPP Bohunice unit-3 and unit-4 with the aim to perform identical thermal and radiation treatment of RPV surveillance specimens as exists in reality.

The total specific activity of the first batch of specimens (sample k716 BM-I with the weight of 25.6 mg) was 3.2×10^7 Bq/g. It is mostly due to presence of ^{60}Co and ^{54}Mn as presented in Table 3 and Fig. 1.

TABLE 3. Activities of the most detected nuclides in RPV-steel specimen k716 BM-I (25.6 mg).

Nuclide	Sb 124	Co 58	Co 60	Cr 51	Fe 59	J 131	Mn 54	Na 24
Activity [Bq]	6438	1673	160750	22622	47952	37660	544790	143
Error	$\pm1\times10^2$	$\pm1\times10^2$	$\pm2\times10^2$	$\pm3\times10^2$	$\pm2\times10^2$	$\pm2\times10^3$	$\pm3\times10^2$	$\pm1\times10^2$
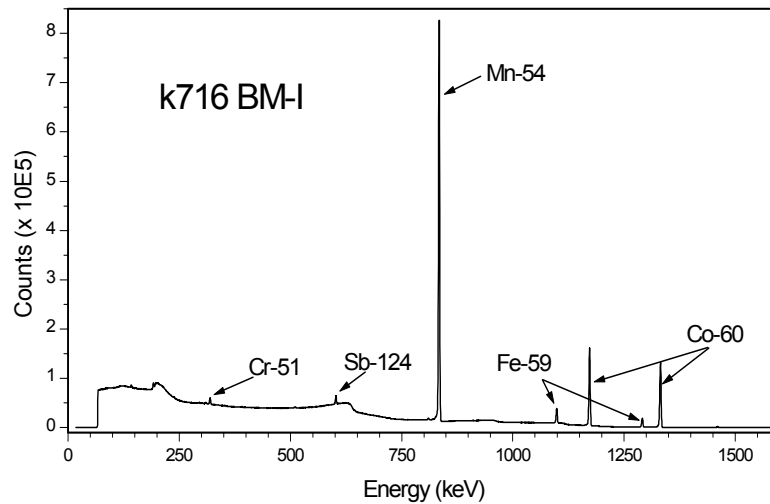
FIG. 1. Gamma spectroscopy spectrum of irradiated RPV-steel specimen 15Kh2MFA (k716-MB-I).

As the most suitable fitting model we used the four components fit with fixed sextet No.2, which corresponds to the pure α-iron with hyperfine field $H_{hf2} = 33.0$ T. MS parameters as areas under sextets (A_x) and hyperfine fields ($H_{hf,x}$) of RPV-steel specimens are selected in Tables 4 and 5. Typical Mössbauer spectra of base metal of RPV specimens after 1-year stay in operated nuclear reactor, treated by the neutron fluency $\Phi(E_n > 0.5 \text{ MeV}) = 7.8\times10^{23}$ m^{-2} are shown in Fig. 2. No doublet component (according to [23] typical for western RPV-steels, assigned to cementite contribution) was identified in spectra. This is most probably due to vanadium presence leading to VC formation in Russian steels.

The most significant change after neutron irradiation is observable in areas under first two components (see Tables 4 and 5). The degradation mechanism of RPV-steel specimens owing to fast neutron bombardment is shown as a decrease of the pure α-iron component presence (fixed in all analysis at $H_{hf,2} = 33.0$ T). The significant decrease (up to 10%) was observed in all specimens. This decrease was balanced by the increased H_{hf1} values of the first component, which can be assigned to the contribution of a complex of atoms (Cr, Ni, Cu, Mn, ...). Comparison of results from both units and between the base and weld material is shown in Fig. 3A–3D.

There were clear differences between base and weld materials, but the behaviour of MS parameters due to irradiation are similar. After relatively intensive jumps of values after the first year of irradiation, these changes do not continue due to increased irradiation treatment and stay almost stable (base metals) or move slightly back (welds). It seems that after the first year of irradiation the effects come to saturation.

TABLE 4. Comparison of RPV-steel specimens in non-irradiated and irradiated state at 3rd unit NPP Bohunice (abbreviations BM-N stand for: base material - not irradiated, BM-I base material – irradiated – numbers of years, WM-N weld material - not irradiated, WM-I weld material – irradiated – numbers of years).

Specimen	A_1 [%]	A_2 [%]	ΔA_1+ [%]	ΔA_2- [%]	A_3 [%]	A_4 [%]	H_{hf1} [T]	H_{hf2} [T]	H_{hf3} [T]	H_{hf4} [T]
k716 BM-N ≡ ZMNF	24.3	35.0			33.3	7.4	33.8	33.0	30.6	28.5
k716 BM-I-1y ≡ ZM1Y	31.6	25.1	7.3	9.9	37.3	6.0	33.7	33.0	30.7	28.6
k723 WM-N ≡ ZKNF	17.2	41.9			34.1	6.8	33.8	33.0	30.6	28.5
k723 WM-I-1y ≡ ZK1Y	23.8	34.0	6.6	7.9	35.3	6.9	33.7	33.0	30.6	28.4
2 years										
k721 BM-N	27.1	30.7			35.2	6.9	33.8	33.0	30.6	28.3
k721 BM-I-2y ≡ ZM2Y	31.1	25.4	4.0	5.3	36.9	6.6	33.7	33.0	30.6	28.1
k725 WM-N	20.5	41.4			30.8	7.3	33.8	33.0	30.7	28.6
k725 WM-I-2y ≡ ZK2Y	21.6	40.7	1.1	0.7	29.6	8.1	33.6	33.0	30.6	28.5
3 years										
k720 BM-N	26.2	32.5			33.7	7.6	33.8	33.0	30.7	28.6
K720 BM-I-3y ≡ ZM3Y	33.4	25.4	7.2	7.1	35.2	6.0	33.7	33.0	30.6	28.1
k728 WM-N	16.5	42.4			35.4	5.7	33.8	33.0	30.6	28.3
k728 WM-I-3y ≡ ZK3Y	19.0	40.1	2.5	2.3	34.6	6.3	33.7	33.0	30.6	28.1
Accuracy	±0.8	±0.8	±0.8	±0.8	±0.8	±0.8	±0.1	±0.0	±0.1	±0.2

TABLE 5. Comparison of RPV-steel specimens in irradiated and non-irradiated state at 4th unit NPP Bohunice.

Specimen	A_1 [%]	A_2 [%]	ΔA_1+ [%]	ΔA_2- [%]	A_3 [%]	A_4 [%]	H_{hf1} [T]	H_{hf2} [T]	H_{hf3} [T]	H_{hf4} [T]
k731 BM-N	24.6	33.3			35.4	6.7	33.8	33.0	30.6	28.3
k731 BM-I-1y	28.4	28.0	3.8	5.3	36.0	7.6	33.7	33.0	30.6	28.2
k735 WM-N	18.1	44.0			31.1	6.8	33.7	33.0	30.6	28.7
k735 WM-I-1y	23.0	38.2	4.9	5.8	32.7	6.1	33.7	33.0	30.6	28.4
2 years										
k733 BM-N	27.1	33.0			34.0	5.9	33.8	33.0	30.6	28.3
k733 BM-I-2y	31.7	27.6	4.6	5.4	34.3	6.4	33.7	33.0	30.6	28.2
k739 WM-N	17.2	46.1			29.1	7.7	33.8	33.0	30.7	28.9
k739 WM-I-2y	20.4	43.0	3.2	3.1	30.2	6.3	33.6	33.0	30.6	28.4
3 years										
k734 BM-N	26.1	36.8			31.5	5.7	33.8	33.0	30.6	28.4
k734 BM-I-3y	31.1	29.7	5.0	7.1	32.2	7.0	33.7	33.0	30.6	28.4
k740 WM-N	17.8	44.9			32.1	5.2	33.8	33.0	30.6	28.6
k740 WM-N-3y	20.5	42.5	2.7	2.4	31.7	5.3	33.7	33.0	30.6	28.1
Accuracy	±0.8	±0.8	±0.8	±0.8	±0.8	±0.8	±0.1	±0.0	±0.1	±0.2
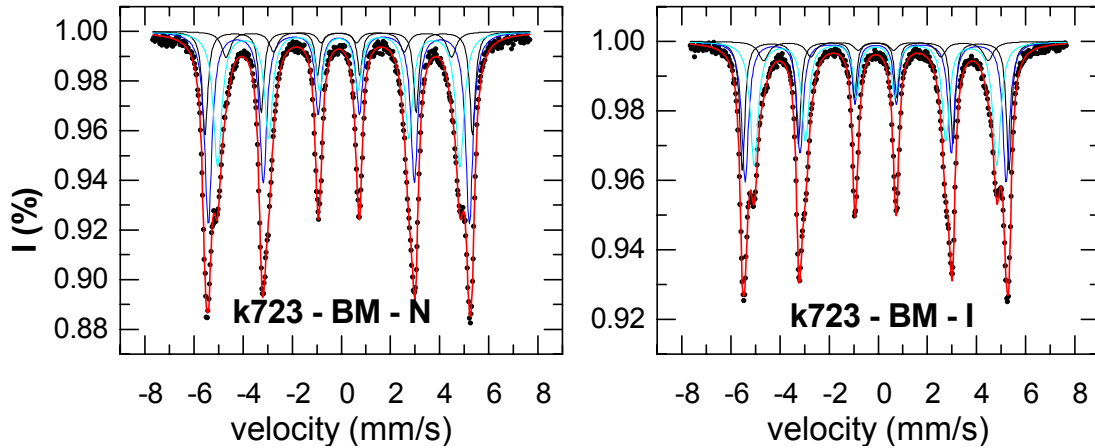
FIG. 2. Comparison of Mössbauer spectra of RPV- base material in non-irradiated and irradiated state.

3A. Unit – base material

3B. Unit – weld

3C. Unit – base material

3D. Unit – weld
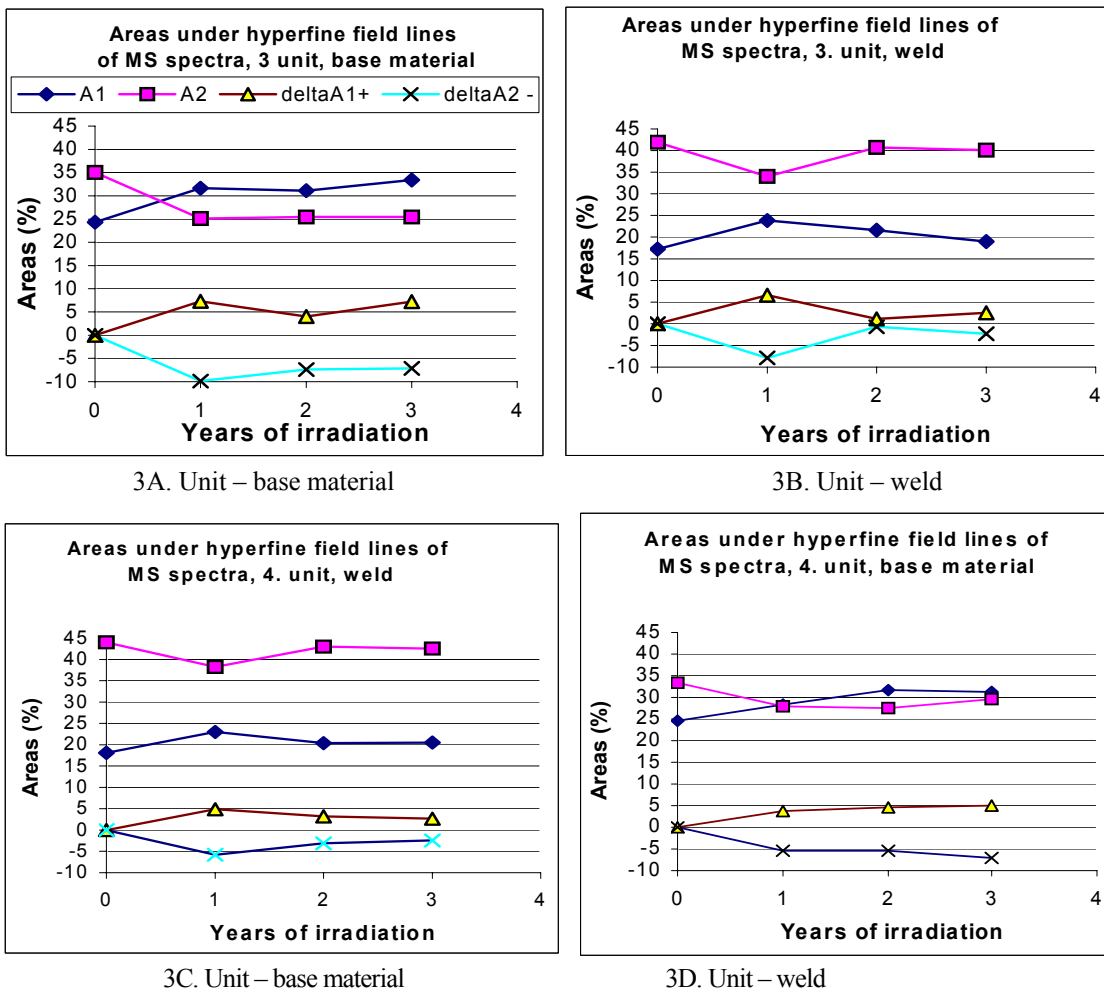
FIG. 3(A-D). Changes in areas under hyperfine field lines of first two sextets of Mössbauer spectra measured on original irradiated RPV-steels from NPP Bohunice (Slovakia) in frame of extended surveillance specimen program. Delta A1+ and delta A2- present increase of first and decrease of second component, respectively.

5.2. PAS Results

According to our previous work and experiences [13, 23-25] a suitable set of RPV steel specimens was selected and prepared for the investigation. In the framework of the "Extended Surveillance Specimen Program" [25, 51], several specimens, prepared originally for Mössbauer spectroscopy

measurements [54], and suitable for PLEPS measurement because of their size (10×10×0.05 mm) and polished surfaces, were selected and measured before and after their irradiation, near the core of the nuclear reactor. The chemical composition and the irradiation conditions of the studied RPV-steel specimens are shown in Table 1 and Table 2. Specimens measured by MS and PAS techniques were identical.

The calculated positron lifetimes for different types of defects in pure iron and different carbides in low alloy Cr-Mo-V steel are shown in Table 6. Experimental results for the mean positron lifetime τ_m after various irradiation treatments are shown in Fig. 4 and Fig. 5. τ_m is plotted versus the mean positron implantation depth. The characteristic decrease of τ_m with increasing positron implantation depth is typical for measurements with a low energy pulsed positron beam. It is due to the back diffusion of positrons to the surface and subsequent trapping at a surface state or in the oxide layer.

TABLE 6. Calculated positron lifetimes for different types of defects in pure iron and different carbides in low alloy Cr-Mo-V steel.

Material	Positron lifetime (ps)	Reference
Fe-bulk	110	[59]
Fe-dislocations	165	[60]
Fe-monovacancy	175	[59]
Fe-divacancy	197	[60]
Fe-3 vacancy cluster	232	[60]
Fe-4 vacancy cluster	262	[60]
Fe-6 vacancy cluster	304	[60]
VC	99	[61]
$V_{0.86}Cr_{0.09}Mo_{0.04}Fe_{0.01}C$	105	[61]
Mo_2C	112	[61]
$Mo_{1.4}Cr_{0.6}C$	116	[61]
Cr_7C_3	107	[61]
$Cr_{23}C_6$	112	[61]
$Mn_{26}C_6$	99	[61]
Fe_3C	101	[61]
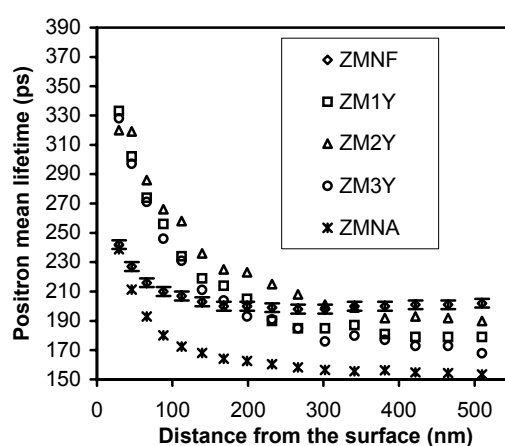
FIG. 4. Comparison of mean lifetimes τ_m of different neutron-irradiated 15Kh2MFA (base metal) steel specimens.
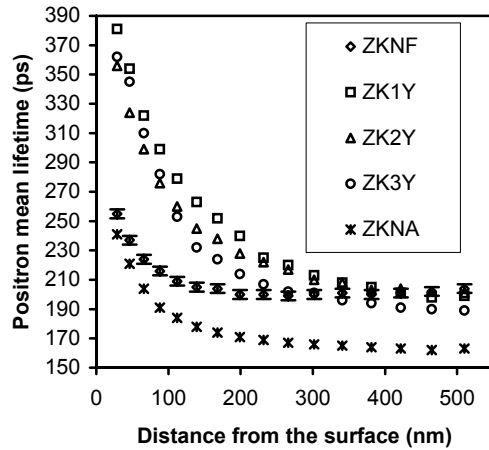
FIG. 5. Comparison of mean lifetimes τ_m of different neutron-irradiated Sv10KhMFT (weld) steel specimens.

Each lifetime spectrum can be well analysed by two lifetime components, which below a depth of about 300 nm remain fairly constant over the full depth range (see Fig. 6 and Fig. 7). The shorter lifetime τ_1 of about 170 ps is the dominant steel component (most likely iron monovacancies or dislocation lines) with an intensity of about 97% in the bulk. The longer lifetime τ_2 with intensity of about 3% or less and a value of about 400-500 ps can be assigned to the contribution of large vacancy clusters. The intensity of this component is surprisingly much higher (up to 10-12 %) for those specimens, which were not thermally treated (reference specimens ZMNF and ZKNF), indicating that large vacancy clusters are already present in the material before irradiation. These ZMNF and ZKNF specimens were annealed for 1 hour in vacuum at 385 ºC and renamed ZMNA and ZKNA (see Table 2 and Figs. 6, 7).
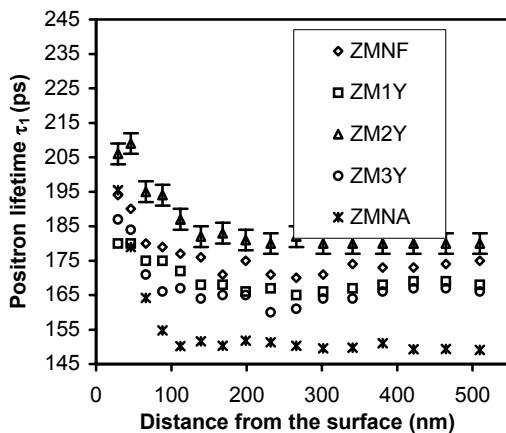
FIG. 6. Comparison of lifetimes τ_1 of RPV steel specimens (base metal) after different neutron irradiation.
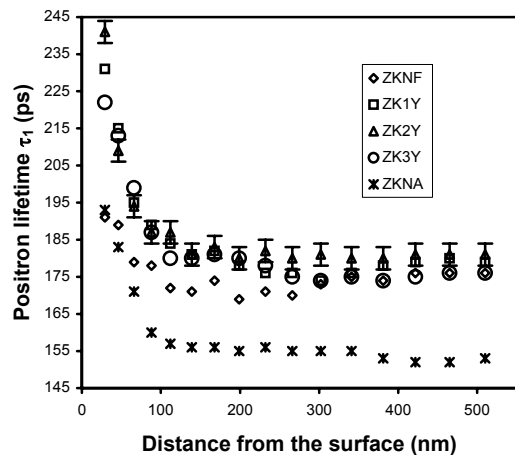
FIG. 7. Comparison of lifetimes τ_1 of RPV steel specimens (weld) after different neutron irradiation.

The interesting results for the irradiated specimens, in respect to the defect structure in the bulk, presented in Fig. 6 and Fig. 7, are the almost constant value of τ_1 for the weld alloy as well as the oscillating behaviour of τ_1 for the base alloy, where the resulting lifetime indicate that after one year and three years irradiation obviously only dislocations are present, whereas after two years of neutron irradiation a mixture of iron mono- and di-vancancies is produced. However, in both base and weld alloys, the concentration of large vacancy clusters is reduced from about 12 percent before irradiation to 3 percent after irradiation. It is very likely that in addition, small irradiation - induced precipitates (probably carbides) with sizes of about 1 to 2 nm [36] developed, which are not so effective for trapping positrons.

Decrease of the mean positron lifetime τ_m after annealing of the non-irradiated specimens (ZMNF and ZKNF) in vacuum at 385 °C for 1 hour was from 200 ± 3 ps to 161 ± 3 ps in the case of base metal (ZM) and from 201 ± 3 ps to 170 ± 3 ps for weld metal (ZK) (see Figs. 4-5).

Of particular interest is the concentration of defects as a function of irradiation dose and thermal treatment. Generally, this effect can be obtained from positron studies only if the bulk lifetime can be resolved from the

shortest lifetime, attributed to annihilation from defects. In the present case of saturation trapping this was impossible. Therefore, from the individual lifetime spectra we can only conclude a total trapping rate κ larger than about 10^{10}s^{-1}.

However, from the variation of the mean lifetime τ_{av} as a function of positron implantation energy, we can estimate κ even in the case of saturation trapping. The problem was fully analysed in [46, 55]. Based on this theory the total defect concentration can be estimated as:

$$c_d = \frac{\kappa}{\kappa_{spec}}$$

In Fig. 8 and Fig. 9 results for the evaluation of κ (trapping rate) as obtained by the procedure described, are presented. For the specific trapping rate κ_{spec} the plausible value $10^{15}(\text{s}^{-1})$ [40] has been assumed. Because of slight surface oxidation, this evaluation of κ results in a systematic underestimate. A lower limit of 10 ns^{-1} for κ may by derived within the framework of the STM since we have observed saturation trapping at defects.
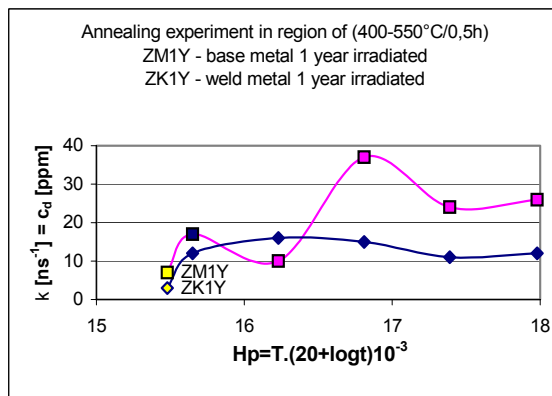
FIG. 8. The total trapping rate κ versus Hollomon-Jaffe´s parameter at isochronal annealed (step 25°C) specimens of base (ZM) and weld (ZK) alloys after 1 year of irradiation in the reactor (fluency of about 7.8×10^{23} m^{-2}). The lower limits for κ, as derived from saturation trapping according to the STM, is 10 ns^{-1}.
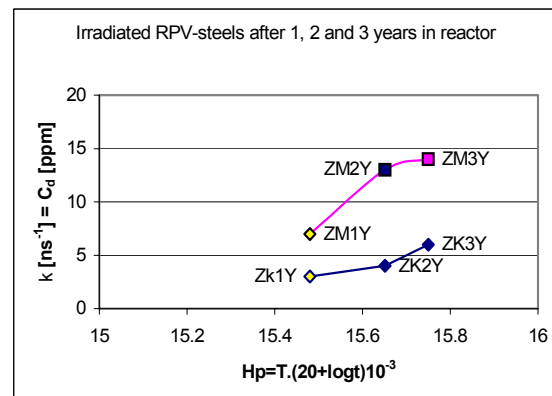
FIG. 9. The total trapping rate κ versus Hollomon-Jaffe´s parameter at RPV specimens from base (ZM) and weld (ZK) alloys after 1, 2 and 3 years residence in reactor irradiation chambers (neutron fluency in the range from 7.8×10^{23} m^{-2} to 2.5×10^{24} m^{-2}). The lower limits for κ, as derived from saturation trapping according to the STM, is 10 ns^{-1}.

According to the results from our measurements performed on different irradiated RPV-steels, the total trapping rate κ in ns^{-1} as well as the total defect concentration c_d (the same values but in ppm) increases slightly for both base and weld materials as a function of the irradiation dose (see Fig. 9). The weld material (Sv10KhMFT) seems to be less sensitive to the changes caused by neutron-irradiation or by post-irradiation heat treatment than the base material (15Kh2MFA) (see Fig. 8). Nevertheless, the differences in the positron trapping rate κ are not too large. It seems reasonable to relate the observed trapping rates with the ones which have been derived for trapping into precipitated carbides from electron microscopic images [20]. Accordingly, in the 15Kh2MFA the trapping rate into chromium carbides (Cr_7C_3, $Cr_{23}C_6$) is predicted as $\kappa_{Cr} = 1.8 \times 10^8$ s^{-1} and into vanadium carbides as $\kappa_{VC} = 2.2 \times 10^{10}$ s^{-1} [20]. Thus precipitated vanadium carbide could indeed account for the observed trapping rates. But on the other hand, as shown by calculations [35], positrons experience a repulsive potential from carbides embedded in an iron matrix. Thus only the defects at the iron-carbide interface could provide an acceptable trapping site for positrons.

The total trapping rate κ and the defect concentration c_d are stable or increase slightly for 15Kh2MFA steel as a function of Hollomon-Jaffe´s parameter which determines the influence of annealing temperature T[K] and time t[s] together [11, 27]. Between 15.5 to 16.5 (corresponding to the temperature region 400 to 450 °C) the defect concentration increases. On the other hand (Fig. 8), in the same range, there is a marked decrease in the lifetime of defects. A simple explanation could be the dissolution of precipitates and defect clusters which would reduce the average size of the defects, and, by the same process, would increase the concentration of the defects.

The annealing effect due to the temperature of about 290 °C and due to the neutron irradiation is in competition with the creation of the new radiation-induced defects.

This finding is supported also by the results from 1D-ACAR and Mössbauer spectroscopy (MS) measurements performed on identical specimens [26, 54].

The steel specimens irradiated for one year were also isochronally annealed for 30 minutes in the temperature range of 400-550 °C in steps of 25 °C. This region was selected according to previous lifetime measurements on the same type of unirradiated material [22]. It was reasonable to start from 400 °C, because the previous isothermal treatment (one year at about 290 °C) is comparable with annealing at 400 °C for 30 minutes. The measured lifetimes of the annealed but non-irradiated specimens indicate that the small vacancy clusters are no longer present but rather a high density of dislocations remains in the sample. Via 3D presentations of PLEPS experimental results, some differences in near surface and bulk regions can be better visualized and understood. There is significant increase of the mean positron lifetime after first level of irradiation, but mostly in the surface-near region. The next long term irradiation at temperature of about 280 ºC induces slight decrease of this parameter. Positron annihilation technique is highly effective for the evaluation of post irradiation heat treatment. Deep PLEPS study of WWEER base and weld metals using PLEPS on neutron fluence level of 7.8×10^{23} m^{-2}, (specimens ZM1Y, ZK1Y). The 2 and 3D presentation of PLEPS results presenting the mean lifetime dependence on irradiation of weld is shown in Fig. 10. Similar behavior of defects creation due to increased neutron fluence was measured also for base metal (presented in other view in Fig. 11). The effectiveness of the annealing process to removing of small defects (mono/di-vacancies or Frenkel pairs) can be followed via significant decrease of parameter τ_1 (see Fig. 12). This figure also shows rapid increase of mentioned small defects in Russian type of RPV steels after about 500 ºC.
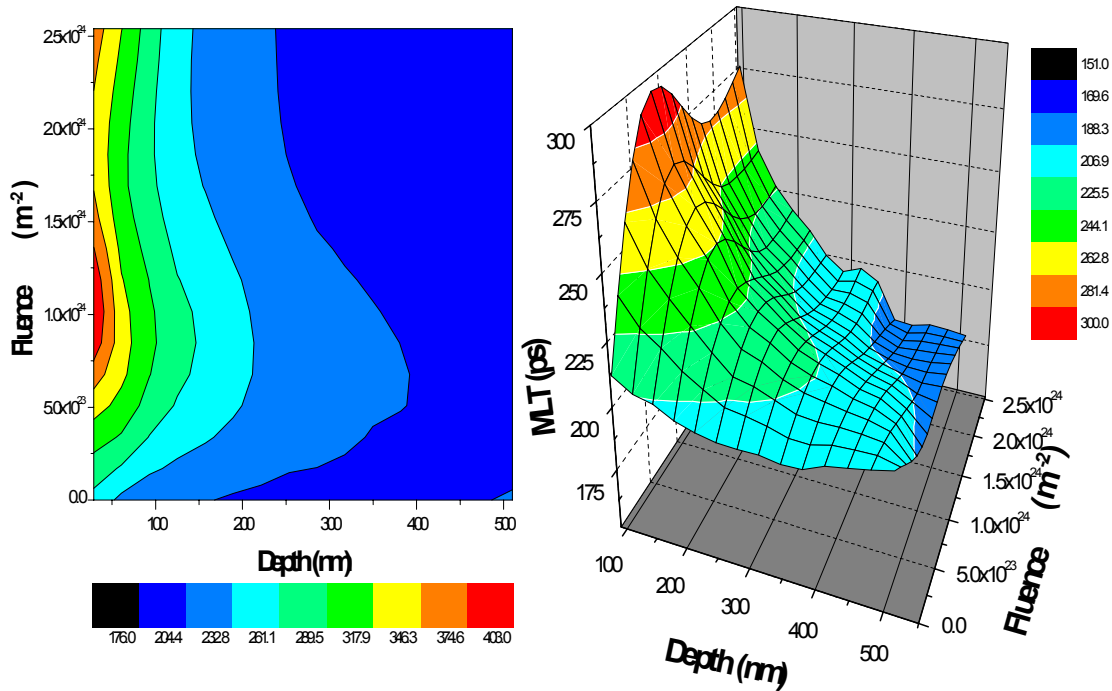
FIG. 10. The 2D and 3D presentation of PLEPS results (MLT) of irradiated Sv-10KhMFT steel (weld metal). The first D about 140 nm were neglected due to possible surface defects.
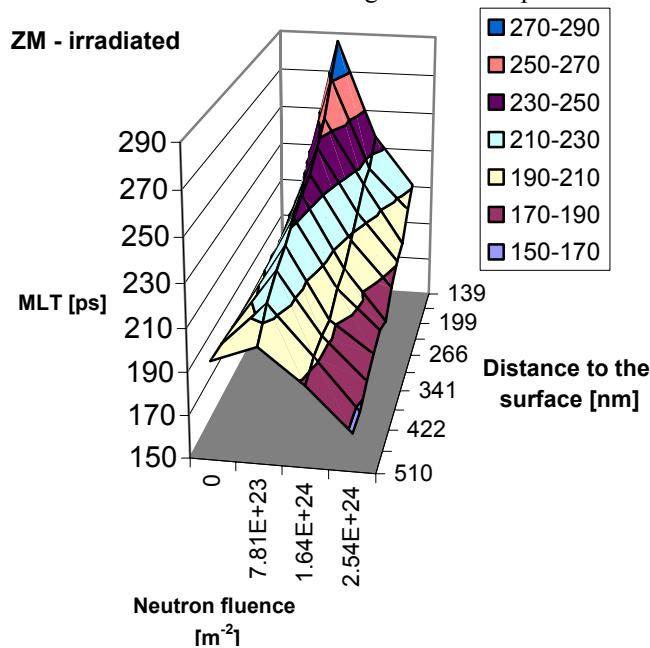
FIG. 11. The 3D presentation of PLEPS results in form of the MLT dependence on neutron fluence. The first about 140 nm were neglected due to possible surface defects.

6. Discussion and Conclusions

Conventional TEM has revealed three kinds of neutron radiation-induced matrix defects in our surveillance specimen, which consists of: black dots, small dislocation loops and fine precipitates, concentrated near dislocations and low-angle boundaries. Non irradiated microstructure of base metal is typical for annealed bainite with coarse carbide M_3C a M_7C_3 and fine carbide MC. Weld metal microstructure is created by acicular and proeutektoid ferrite and the heat affected zone (HAZ) is created by acicular mixture martensite, self-tempered martensite and down bainite. Dislocation structure of base metal, weld metal and heat affection zone is locally markedly changed. BM dislocation structure is created by dislocation

net, but also simple dislocation configurations, which are probably anchored by MC carbide [24]. Dislocation structure is more homogeneous in WM than in BM. No micro voids were found in any surveillance specimen investigated by TEM after irradiation. The weld joint dislocation density of analyzed steel is after five-year irradiation in comparison with former exposures invariable. Dislocation substructure is evidently recovered in base metal after irradiation, the number of two-dimensional networks has increased, networks are more entire as in non-irradiation state. Locations with upper density account for specific

description of dislocations configurations too. Dislocation loops and fine precipitates density little by little decrease, relaxation, after the first year irradiation, but density increases and achieves saturation state after two, three and five years of irradiation. Their size increases and their visibility grow with increasing neutron fluence. Decoration of original dislocations with radiation-induced defects is rather general phenomenon in neutron-irradiated materials. Decoration of dislocations with a defects population probably plays a key role in irradiation induced hardening.
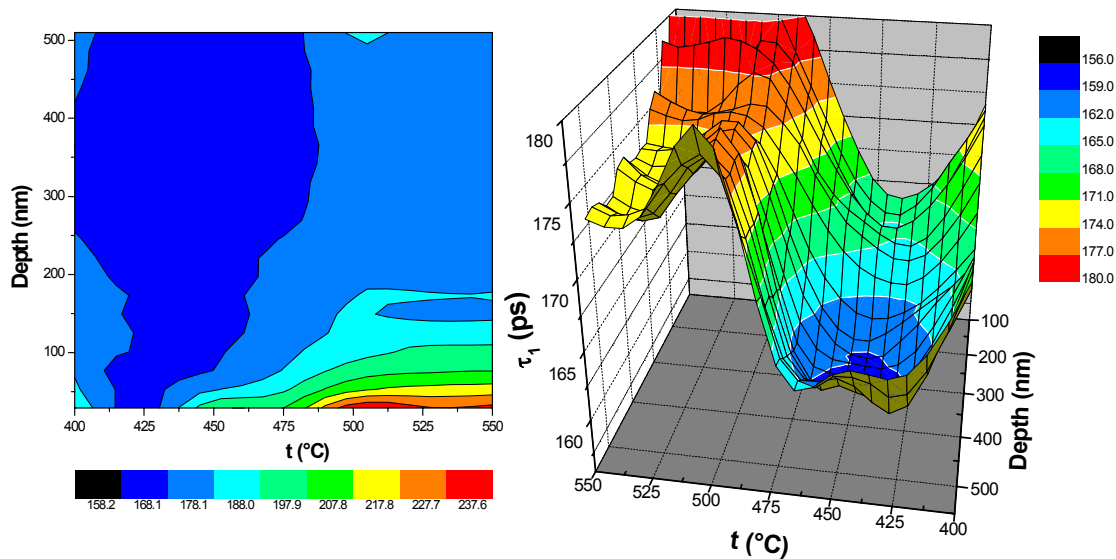
FIG. 12. The 2D and 3D presentation of PLEPS results (Tau1) of irradiated and annealed Sv-10KhMFT steel (weld metal) to level of neutron fluence 1.25×10^{24} m^{-2}. The first about 140 nm were neglected due to possible surface defects.

Both vacancy and interstitial point defects are expected to be mobile in the temperature range of most operating pressure vessels. However, they are also expected to interact with solute atoms. The key interstitial impurity in Russian RPV steel is Carbon [11, 27]. The partial or complete trapping of self-interstitial by C solutes will cause heterogeneous cluster nucleation and a fine cluster distribution. Further, in steels containing residual levels of elements such as copper, which are in super-saturated solution, radiation-enhanced diffusion will occur at these temperatures, which leads to the formation of small clusters, which can again harden the matrix. Generally, the thermal treatment together with neutron irradiation lead to a microstructure consisting of small clusters (< 5 nm in diameter) which create

obstacles to the free movement of dislocations thereby producing an increase in the yield stress, hardness and the ductile-brittle transition temperature of the material [8, 36].

Mössbauer spectroscopy precisely identifies the close environment of Mössbauer nucleus (Fe). Although, this method is very suitable for materials containing Fe, an interpretation of results is very difficult in complex steels. Using MS, it is possible to observe changes in hyperfine fields of atoms in the lattice and according to these to evaluate the precipitation of some elements (mainly in the form of carbides [31]). Their relative areas are close to the theoretical values calculated from a random distribution model of impurities in a b.c.c. structure (5% of 12 elements in total). Results

85

confirmed MS sensitivity to detect also small differences in chemical composition or preparation technology of RPV steel samples. In comparison with Western types of RPV steels such as A533 C1.1 and A508 C1.3, the doublet fraction ascribed as Mn and/or Cr-substituted cementite is completely absent in 15Kh2MFA. Here probably mainly Cr23C6, Cr7C3 and VC carbides are formed. [34].

Significant differences in MS parameters between the RPV base and weld materials can be explained by different chemical compositions and/or different preparation technology and were observed also in the past [29, 31, 34]. The trend in the changes due to irradiation is almost the same in both materials. It seems that the expected changes in material microstructure (precipitation of elements like Cu or Cr mainly in carbides to the surface) were performed mainly during the initial period (1-year stay in irradiation containers in operating conditions by "speed factor" of about 10). These results confirm that the close environment of Fe atoms in the b.c.c. lattice of RPV steels remains after initial changes, almost stable and perhaps could be correlated with the trend of ductile-brittle transition temperature (DBTT) curve obtained from mechanical tests or with the defect density curve obtained from the transmission electron microscopy studies. With increased neutron fluence (up to $\Phi(E_n >$ 0.5 MeV) $= 1\times10^{25}$ m^{-2}) the dislocation density number as well as the average defect diameter remain stable after an initial increase of about 20-30% [28].

On the other hand, the isochronal annealing of 2 selected irradiated specimens performed at 400, 475 and 520 °C did not cause return of the MS parameters to the starting positions. It means that the radiation-induced changes observable in MS spectra were not re-annealed in such a complete way as the re-annealing of point defects observed by TEM [18, 28].

The PLEPS technique enables the depth profiling from the surface to a specimen depth of about 500 nm. Therefore, the micro structural changes in very small and thin specimens could be studied. Thanks to this technique and very small volume of specimens, the disturbing contribution of ^{60}Co radiation in the PAS lifetime spectra were reduced to a minimum. In our case, identical specimens were used for PAS and MS study. Such approach seems to be optimal due to possible inhomogenities in different specimens from the same steels. Nevertheless, there exist many open questions and there is a need for further investigation. Interpretation of PAS and MS results is neither easy nor straightforward. Both techniques are very sensitive to sample preparation and handling.

It was shown that MS as well PLEPS can see the formation of solute clusters during irradiation of RPV steels, resulted in depletion of Cu and P in the matrix in the first period of irradiation. Some alloying elements (for example Ni) can slightly retard this depletion [56]. After this first period, both techniques registered no significant changes connected to increased neutron treatment. In the contrary, the positron lifetimes decreased probably due to long-term thermal treatment on the level of 280 °C. Using PLEPS, the most effective region (450-470 °C) of thermal treatment was clearly shown at base as well as weld metals. Positron annihilation techniques can be applied for the development of new types of steels with well-defined parameters (materials for fusion reactors, etc.) or by the evaluation of the effectiveness of post-irradiation thermal treatments [57]. Application of a scanning positron microscope in the RPV-steel investigation would be surely one of the ways in the future [58].

The results from the present extensive study of RPV surveillance specimens indicate that MS and PAS could be useable techniques for the evaluation of some microstructural changes in RPV-steels and, in combination with other spectroscopic methods can contribute to an increase of NPPs operational safety and lifetime prediction. However, neither this method is a magic wand solving all substantial questions in neutron embrittlement and material ageing. This investigation will continue also in the next period and specimens treated in reactor up to 10 years will be studied. Such loaded specimens will be equivalent to real RPV steel after more than 50 years of operation and will be interesting for the RPV lifetime management.

Acknowledgement

References

[1] Davies, L.M., Int. J. Press. Ves. & Piping, 76 (1999) 163.

[2] Nikolaev, Y.A., Nikolaeva, A.V., Kryukov, A.M., Shtrombakh, Y.I. and Platonov, P.A., Proc. of the TACIS Workshop on the RPV Life Predictions, PCP3-ENUCRA-D4 (2000).

[3] Ghoniem, M.M. and Hammad, F.H., Int. J. Press. Vess. & Piping, 74 (1997) 189.

[4] Kohopaa, J. and Ahlstrand, R., Int. J. Press. Vess. & Piping, 76 (2000) 575.

[5] Debarberis, L., von Estorff, U., Crutzen, S., Beers, M., Stamm, H., de Vries, M.I. and Tjoa, G.L., Nucl. Eng. Des. 195 (2000) 217.

[6] U.S. NRC Regulatory Guide 1.99, Rev.1, (1977).

[7] Suzuki, K., IAEA report, IWG-LMNPP-98/3, (1998).

[8] Grosse, M., Denner, V., Böhmert, J. and Mathon, M.H., J. Nucl. Mater. 277 (2000) 280.

[9] Koutsky, J. and Kocik, J., "Radiaton damage of structural materials", ed. Academia Prague, (1994).

[10] Phythian, W.J. and English, C.A., J. Nucl. Mater. 205 (1993) 162.

[11] Brauer, G., Liszkay, L., Molnar, B. and Krause, R., Nucl. Eng. & Desg. 127 (1991) 47.

[12] Pareja, R., De Diego, N., De La Cruz, R.M. and Del Rio, J., Nucl. Technol. 104 (1993) 52.

[13] Lopes Gil, C., De Lima, A.P., Ayres De Campos, N., Fernandez, J.V., Kögel, G., Sperr, P., Triftshäuser, W. and Pachur, D., J. Nucl. Mater. 161 (1989) 1.

[14] Slugen, V., Zeman, A., Petriska, M. and Krsjak, V., Applied surface science, 252 (2006) 3309.

[15] Valo, M., Krause, R., Saarinen, K., Hautojärvi, P. and Hawthorne, R., ASTM STP 1125, Stoller, Philadelphia, (1992).

[16] Hartley, J.H., Howell, R.H., Asoka-Kumar, P., Sterne, P.A., Akers, D. and Denison, A., Appl. Surf. Sci. 149 (199) 204.

[17] Becvar, F., Cizek, J., Lestak, L., Novotny, I., Prochazka, I. and Sebesta, F., Nucl. Instr. Meth. A 443 (2000) 557.

[18] Miller, M.K., Russel, K.F., Kocik, J. and Keilova, E., J. Nucl. Mater. 282 (2000) 83.

[19] Cizek, J., Becvar, F. and Prochazka, I., Nucl. Instr. Meth. A 450 (2000) 325

[20] Cizek, J., Prochazka, I., Kocik, J. and Keilova, E., phys. stat. sol. (a) 178 (2000) 651.

[21] Van Hoorebeke, L., Fabry, A., van Walle, E., Van de Velde, J., Segers, D. and Dorikens-Vanpraet, L., Nucl. Instr. Meth. A 371 (1996) 566.

[22] Ghazi-Wakili, K., Zimmermann, U., Brunner, J., Tipping, P., Waeber, W.B. and Heinrich, F., Phys. Stat. Sol. (a) 102 (1987) 153.

[23] Slugen, V., Segers, D., De Bakker, P.M.A., DeGrave, E., Magula, V., Van Hoecke, T. and Van Waeyenberge, B., J. Nucl. Mater. 274 (1999) 273.

[24] Slugen, V. and Magula, V., Nucl. Eng. Desg. 186(3) (1998) 323.

[25] Slugen, V., De Grave, E. and Segers, D., Int. J. Nuclear Energy Science and Technology, 1(1) (2004) 20.

[26] Slugen, V., Hascik, J., Gröne, R., Bartik, P., Zeman, A., Kögel, G., Sperr, P. and Triftshäuser, W., Material Science Forum, 47 (2001) 363.

[27] Magula, V. and Janovec, J., Ironmaking and Steelmaking, 21 (1994) 64.

[28] Kocik, J., Keilova, E., Cizek, J. and Prochazka, I., Proc. of 9th Int. Conf. on Metallurgy METAL 2000, (CD-ROM), Ostrava, Czech Republic, Tanger Ltd., (2000), paper No.719.

[29] Lipka, J., Hascik, J., Slugen, V., Kupca, L., Miglierini, M., Gröne, R., Toth, I., Vitazek, K. and Sitek, J., Proc. Int. Conf. ICAME'95, Vol. 50, I. Ortalli (ed.), SIF, Bologna, (1996), 161.

[30] Cohen, L., "Application of Mössbauer spectroscopy". Volume II. (Academic Press, New York, 1980).

[31] Brauer, G., Matz, W. and Fetzer, Cs., Hyperfine Interaction, 56 (1990) 1563.

[32] Amaev, A.D., Dragunov, Yu.G., Kryukov, A.M., Lebedev, L.M. and Sokolov, M.A., Proc. of IAEA specialists meeting of RPV embrittlement, Plzeň, (1986).

[33] Slugen, V., "Mössbauer spectroscopy in material science", In: M. Miglierini and D. Petridis (eds.), 119-130, (Kluwer Academic Publishers, Netherlands, 1999).

[34] De Bakker, P., Slugen, V., De Grave, E., Van Walle, E. and Fabry, A., Hyperfine Interaction. 110 (1997) 11.

[35] Puska, M.J., Sob, M., Brauer, G. and Korhonen, T., Phys. Rev. B, 49 (1994) 10947.

[36] Böhmert, J. and Grosse, M., Proc. of Jahrestagung Kerntechnik 1998, ed. Inforum Verlag, Bonn, (1998), 741.

[37] Davies, M., Kryukov, A., English, C., Nikolaev, Y. and Server, W., ASTM STP 1366 (2000).

[38] Nagai, Y., Tang, Z., Hasegawa, M., Kanai, T. and Saneyasu, M., Phys. Rev. B, 63 (2001) 131110.

[39] Mukouda, I. and Shimomura, Y., Mat. Sci & Eng. 190 (2001) A309.

[40] Brandt, W., "Positron Annihilation", A.T. Stewart and L.O. Roelling (eds.), (Academic Press, New York, 1967), p.155.

[41] Frank, W. and Seeger, A., Appl. Phys. 3 (1974) 61.

[42] Seeger, A., Appl. Phys. 4 (1974) 183.

[43] Nieminen, R.N., Laakkonen, J., Hautojärvi, P. and Vehanen, A., Phys. Rev. B, 19 (1979) 1397.

[44] Frieze, W.E., Lynn, K.G. and Welch, D.O., Phys. Rev. B, 31 (1985) 15.

[45] Britton, D.T., J. Phys.: Condens. Matter, 3 (1991) 681.

[46] Kögel, G., Appl. Phys. A, 63 (1996) 227.

[47] Sperr, P., Kögel, G., Willutzki, P. and Triftshäuser, W., Applied Surface Science, 116 (1997) 78.

[48] Bauer-Kugelmann, W., Sperr, P., Kögel, G. and Triftshäuser, W., Mater. Sci. Forum, 529 (2001) 363.

[49] Dai, G.H., Moser, P. and Van Duysen, J.C., Mater. Sci. Forum, 941 (1992) 105.

[50] Prochazka, I., Novotny, I. and Becvar, F., Mater. Sci. Forum, 772 (1997) 255.

[51] Kupca, L. and Beno, P., Nucl. Eng. & Desg. 196 (2000) 81.

[52] Gröne, R., Hascik, J., Slugen, V., Lipka, R., Pietryzk, P. and Vitazek, K., Nucl. Instr. & Meth. in Phys. Res. B, 129 (1997) 284.

[53] Slugen, V., Hascik, J. and Gröne, R., International J. of Applied Electromagnetics and Mechanics, 11 (2000) 39.

[54] Slugen, V., Lipka, J., Toth, I. and Hascik, J., NTD&E Int. 35(8) (2002) 511.

[55] Slugen, V., Kögel, G., Sperr, P. and Triftshäuser, W., Appl. Surf. Sci. 194 (1-4) (2002) 150.

[56] Zeman, A., Debarberis, L., Kocik, J., Slugen, V. and Keilova, E., J. of Nuclear Materials, 362 (2007) 259.

[57] Slugen, V., Kuriplach, J. and Ballo, P., Nuclear Fusion, 44 (2004) 93.

[58] David, A., Kögel, G., Sperr, P. and Triftshäuser, W., Phys. Rev. Lett. 87 (2001) 067402.

[59] Hautojärvi, P., Pöllönen, L., Vehanen, A. and Yli-Kauppila, J., J. Nucl. Mater. 114 (1983) 250.

[60] Vehanen, A., Hautojärvi, P., Johansson, J., Yli-Kauppila, J. and Moser, P., Phys. Rev. B, 25 (1982) 762.

[61] Brauer, G., Sob, M. and Kocik, J., Report ZfK-647, (1990).

[62] Slugen, V., Nuclear engineering and design, 235 (2005) 1961.

[63] Zeman, A., Debarberis, L., Slugen, V. and Acosta, B., Applied surface science 252(9) (2006) 3290.